Optical and Quantum Electronics (2023) 55:1031
https://doi.org/10.1007/s11082-023-05360-0

Optimization of waveguide parameters for minimization of the sensitivity temperature dependence for the SiO_2:TiO_2 planar waveguide optical sensor

Abdelbaki Cherouana[1] · Salim Benaissa[1] · Abdelhalim Bencheikh[2] · Idris Bouchama[3,4]

Received: 11 June 2023 / Accepted: 30 August 2023 / Published online: 21 September 2023

Abstract
This study focuses on investigating how changes in temperature affect the sensitivities of an optical sensor that uses a SiO_2:TiO_2 planar waveguide, with particular emphasis on the fundamental modes sensitivities. The results showed that, by accurately determining the appropriate core thickness for each set of physical parameters of the waveguide, we not only increased the sensitivity, but also extended its stabilization range with respect to the temperature. The best results, in terms of values and stabilities of the sensitivities were obtained for a high refractive index of the core and selecting a measurand refractive index closest to that of substrate. As regards the geometrical parameters, the most favorable results can be attained for the core thicknesses located between the thickness corresponding to the maximum sensitivity at room temperature and the cut-off thickness of the TM_0 mode, the sensitivity remain relatively stable at the vicinity of 0.41. However, for the monomode structure, the best results can be achieved for the core thicknesses situated between the thickness corresponding to the maximum sensitivity at room temperature and twice the cut-off thickness of the TE_0 single mode, the average sensitivity is relatively constant at around 0.35.

Keywords Optical sensor · SiO_2:TiO_2 planar waveguide · Temperature dependence · Sensitivity · Waveguide parameters

✉ Abdelbaki Cherouana
acherouana@cdta.dz

[1] Research Unit in Optics and Photonics, Center for Development of Advanced Technologies (CDTA), University of Ferhat Abbas Sétif 1, Algiers, Algeria

[2] Department of Electromechanics, University of Mohamed El Bachir El Ibrahimi, Bordj Bou Arreridj, Algeria

[3] Department of Electronic, University of Mohamed BOUDIAF, M'sila, Algeria

[4] Research Unit on Emerging Materials (RUEM), University Ferhat Abbas Sétif 1, Sétif, Algeria

1 Introduction

The principle sensing, in many optical waveguide based sensors, is the interaction of the medium surrounding the waveguide with the evanescent field of the propagated wave. Therefore, some of the properties of this latter (wavelength, amplitude or polarization) change and by monitoring these changes, the analyte of the concerned medium can be detected (Uniyal et al. 2023). In fact, different techniques for implementing optical waveguide thin films have been established, that involve chemical, physical, and refractive index modification methods. The simplest and most effective method to be used is the sol–gel method and dip coating technique (Butt et al. 2022a). In such technique, the refractive indices and thickness of the waveguiding film can be controlled by adjusting the molar ratio of the components and the annealing temperature, in addition to the self-stopping precursors and solvents (Butt et al. 2022b). Moreover, optical waveguide based sensors can be made from various materials depending on the purposes they serve. Recently, plasmonic refractive index sensors and nanosensors have attracted significant research interest. Therefore, a concentric double-ring resonator based MIM (Metal–Insulator–Metal) waveguides, was presented for glucose sensing capability (Farhad et al. 2020). A MIM refractive index sensor based on concentric triple ring resonator, was proposed for cancer biomarker and chemical concentration detection (Infiter et al. 2022). A cog-shaped MIM refractive index sensor studded with gold nanorods was numerically studied for temperature sensing of multiple analytes (Kazi et al. 2021a). Furthermore, (Kazi et al. 2021b) have presented a MIM nanosensors based on three circular rings for Gas-sensing and label-free detection of biomaterials. (Infiter et al. 2021a) have proposed (MIM) pressure sensor loaded with arrays of silver nanorods. In addition to MIM refractive index sensor, alternative materials based refractive index sensors have been proposed, such as, Titanium Nitride based refractive sensor (Infiter et al. 2021b), and dielectric-metal-dielectric (DMD) waveguides based nanosensors (Farhad et al. 2017).

As plasmonic refractive index sensors, optical sensors based on dielectric waveguides are well suited for chemical, gas, environmental and biological sensing. In particularly, the use of optical sensors in harsh environments is paramount. For example, high temperature gas sensors are mainly designed to solve gas detection and monitoring problems with a high operating temperature environment, such as gas turbine, nuclear power plants and automobile internal combustion engine emission (Ghosh et al. 2019; Dhall et al. 2021; Karker et al. 2017). In reality, metal oxide-based gas sensors such as SnO_2, WO_3, ZnO, NiO or CuO operate mostly at moderate temperatures. However, those based on Titanium dioxide (TiO_2) are capable to operate above 500 °C (Fomekong and Saruhan 2021). Titanium dioxide attracts the researcher's attention around the world, because of its unique properties. In fact, TiO_2 is a non-toxic solid inorganic substance, thermally and chemically stable, non-flammable, transparent and has a large refractive index (Parrino and Palmisano 2021).

On the other hand, the use of titanium dioxide embedded in silica matrix, make produced Silica–Titania waveguide systems, highly attractive. In fact, Silica–Titania waveguides have very low propagation losses, very good stability and operation in both visible and near-infrared wavelength ranges (Karasinski et al. 2011; Butt et al. 2021a, b; Morosanova 2012; Morosanova 2016; Chiavaioli et al. 2015 and Islam et al. 2020). Moreover, a numerical analysis of Silica–Titania based reverse rib waveguide with rounded and vertical side, has appeared similar modal characteristics at the operational wavelength 1550 nm (Butt et al. 2021a, b). These properties make Silica–Titania systems suitable for integrated

photonics. For example, a 1 × 2 demultiplexer for telecommunication wavelength 1550 nm and 1310 nm was proposed on silica–titania platform. This study can further open the possibilities of designing 1 × N demultiplexing devices (Butt et al. 2023).

In addition to that, refractive indices and thickness of Silica–Titania films are function of temperature. Hence, these films are promising materials for some integrated optical devices, whose, their operation principle is based on the temperature dependence of the effective refractive index of the guided modes (Nikolaev et al. 2012a,b; Pavlov et al. 2014; Pavlov et al. 2013; Nikolaev et al. 2018 and Chekhlova et al. 2006). Mainly, Silica–Titania planar waveguides systems are highly suitable for optical sensing applications (Butt et al. 2021a, b; Morosanova 2012; Morosanova 2016; Islam et al. 2018; Tiefenthaler and Lukosz 1989).

Sensitivity is the most important parameter of a planar optical sensor. In order to obtain a high value of the sensitivity and a better stability of this one as the temperature increases, our objective revolves around identifying specific waveguide parameters that minimize the temperature-dependent changes in sensitivity for the SiO_2:TiO_2 planar waveguide optical sensor. The study focuses, mainly, on the fundamental guided modes. Noting that, the variation of the sensitivity as a function of the temperature follows the temperature dependence of the effective refractive index, which follows the temperature dependence of the physical and geometrical parameters of the waveguide (Nikolaev et al. 2018).

2 Theoretical modeling

2.1 Dispersion equations under temperature dependence of the waveguide parameters

Figure 1 represents a schematic illustration of the investigated planar waveguide based optical sensor under temperature variation (T). The slab waveguide is composed of SiO_2:TiO_2 core deposited on a substrate of AF45 glass.

The dispersion equations of the planar waveguide, for both TE and TM modes, are obtained using the appropriate Maxwell equations and bouandary conditions, with considering two factors: the temperature dependence of the refractive indices of the core and substrate, $n_f(T)$, $n_s(T)$, respectively, and the temperature dependence of the film thickness, $d(T)$, as given by several references, such as (Pavlov et al. 2013):

$$k_0 d(T)\sqrt{n_f^2(T) - N(T)^2} = arctan\left(\sqrt{\frac{N(T)^2 - n_s^2(T)}{n_f^2(T) - N(T)^2}}\right) + arctan\left(\sqrt{\frac{N(T)^2 - n_c^2}{n_f^2(T) - N(T)^2}}\right) + m\pi \tag{1}$$

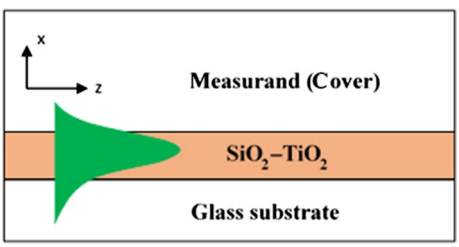

Fig. 1 Evanescent wave-based SiO_2:TiO_2 planar waveguide optical sensor

For TE modes and

$$k_0 d(T)\sqrt{n_f^2(T)-N(T)^2} = arctan\left(\frac{n_f^2(T)}{n_c^2}\sqrt{\frac{N(T)^2-n_c^2}{n_f^2(T)-N(T)^2}}\right) + arctan\left(\frac{n_f^2(T)}{n_s^2(T)}\sqrt{\frac{N(T)^2-n_s^2(T)}{n_f^2(T)-N(T)^2}}\right) + m\pi \quad (2)$$

For TM modes.

Where n_c is the refractive index of the cover or measurand, m is the mode order, and $N(T)$ is the effective refractive index of the guided mode, as a function of the temperature. k_0 is the wave number in the vacuum.

To calculate the temperature dependences of the effective refractive index of Silica–Titania slab waveguide, we will employ numerical method to solve the dispersion equations, considering the temperature dependence of the waveguide parameters. These calculated effective refractive indices will then be utilized to determine the temperature dependence of the optical sensor sensitivities.

The temperature dependences of $n_f(T)$, $n_s(T)$ and $d(T)$ are given by the following empirical expressions, taken from (Nikolaev et al. 2012b) and (Sainit et al. 1994):

$$n_f(T) = -2.047 \times 10^{-7} \times T^2 - 2.185 \times 10^{-5} \times T + n_f \quad (3)$$

$$n_s(T) = 1.5254 - 1.23 \times 10^{-6} \times T \quad (4)$$

$$d(T) = d_0 \times \left(1.168 \times 10^{-6} \times T^2 - 1.838 \times 10^{-5} \times T + 1\right) \quad (5)$$

where n_f and d_0 are the refractive index and thickness of the core at the temperature 0 °C, respectively.

In our study, we will examine both multimode and single mode structures. For the multimode structure, we will consider two cases: one where only the fundamental modes TE_0 and TM_0 propagate and another where the TM_1 mode can also propagates. Therefore, conditions of these three cases need to be determined.

2.2 Multimode condition

The multimode propagation exists if the cut-off thicknesses for the mth guided TM mode satisfies the following condition, deduced from (Chin 2007):

$$\frac{arctan\left(\sqrt{\frac{n_f^4 n_s^2 - n_c^2}{n_c^4 n_f^2 - n_s^2}}\right) + m\pi}{k_0\sqrt{n_f^2 - n_s^2}} \le d_{cut-off}; for\ TM\ modes \quad (6)$$

$$\frac{arctan\left(\sqrt{\frac{n_s^2 - n_c^2}{n_f^2 - n_s^2}}\right) + m\pi}{k_0\sqrt{n_f^2 - n_s^2}} \le d_{cut-off}; for\ TE\ modes \quad (7)$$

The condition, for which only fundamental modes, TE_0 and TM_0 propagate, can be, also deduced from (Chin 2007), as:

$$\frac{arctan\left(\sqrt{\frac{n_f^4 n_s^2 - n_c^2}{n_c^4 n_f^2 - n_s^2}}\right)}{k_0\sqrt{n_f^2 - n_s^2}} \leq d_{cut-off} < \frac{arctan\left(\sqrt{\frac{n_s^2 - n_c^2}{n_f^2 - n_s^2}}\right) + \pi}{k_0\sqrt{n_f^2 - n_s^2}} \tag{8}$$

Noting that for multi-mode propagation, the condition of the mth guided modes sufficient, because their cut-off thicknesses are always greater than those of TE modes of the same order.

2.3 Single mode condition

It is possible to propagate a single fundamental mode TE_0 in the case where d satisfies the cut-off thicknesses condition, deduced from (Chin 2007):

$$\frac{arctan\left(\sqrt{\frac{n_s^2 - n_c^2}{n_f^2 - n_s^2}}\right)}{k_0\sqrt{n_f^2 - n_s^2}} \leq d_{cut-off} < \frac{arctan\left(\sqrt{\frac{n_f^4 n_s^2 - n_c^2}{n_c^4 n_f^2 - n_s^2}}\right)}{k_0\sqrt{n_f^2 - n_s^2}} \tag{9}$$

2.4 Temperature dependence of the sensitivity of the slab waveguide based sensor

Sensitivity is the change of the sensor output signal in response to unit change in a property of the sensor (the concentration of an analyte surrounded the surface of the sensor). A parameter defines the ability of a sensor to transduce an input signal to an output one. The sensitivity is function of the substance to be detected and the kind of the waveguide transducer. The sensitivity is deduced from the expression:

$$S = \left(\frac{\partial n_c}{\partial N(T)}\right)^{-1} \tag{10}$$

By differentiating the characteristics Eqs. (1) and (2) and considering the last Eq. (10), we get:

$$S_{TE} = \sqrt{\frac{1 - a_c(T)}{1 - X(T)}} \frac{X(T)}{a_c(T)\sqrt{a_c(T) - X(T)}} \frac{1}{\left[K(T) + \frac{1}{\sqrt{a_s(T) - X(T)}} + \frac{1}{\sqrt{a_c(T) - X(T)}}\right]} \tag{11}$$

For TE modes, and

$$S_{TM} = \frac{\left[2\sqrt{\frac{1-X(T)}{1-a_c(T)}} - \sqrt{\frac{1-a_c(T)}{1-X(T)}}\right] \frac{X(T)(1-a_c(T))}{a_c(T)\sqrt{(a_c(T)-X(T))}[1-X(T)(2-a_c(T))]}}{\left[K'(T) + \frac{(1-a_c(T))}{\sqrt{(a_c(T)-X(T))}[1-X(T)(2-a_c(T))]} + \frac{(1-a_s(T))}{\sqrt{(a_s(T)-X(T))}[1-X(T)(2-a_s(T))]}\right]} \tag{12}$$

For TM modes.

Where the following parameters are function of the temperature

$$K(T) = \frac{arctan\sqrt{\frac{a_s(T)-X(T)}{X(T)}} + arctan\sqrt{\frac{a_c(T)-X(T)}{X(T)}} + m\pi}{\sqrt{X(T)}} \tag{13}$$

$$K'(T) = \frac{arctan\frac{1}{1-a_c(T)}\sqrt{\frac{a_c(T)-X(T)}{X(T)}} + arctan\frac{1}{1-a_s(T)}\sqrt{\frac{a_s(T)-X(T)}{X(T)}} + m\pi}{\sqrt{X(T)}} \tag{14}$$

$$a_c(T) = 1 - \frac{n_c^2}{n_f^2(T)}; X(T) = 1 - \frac{N^2(T)}{n_f^2(T)}\ a_s(T) = 1 - \frac{n_s^2(T)}{n_f^2(T)} \tag{15}$$

3 Results and discussions

We have developed a Matlab program to calculate the temperature dependence of the sensitivity and the effective refractive index for both TE and TM modes in a SiO_2:TiO_2 planar waveguide based optical sensor. This temperature dependence follows the temperature dependence of the refractive indices of the waveguiding film and substrate, as well as the temperature dependence of the waveguiding film thickness. Our focus is on the TE_0 and TM_0 modes, due to their higher sensitivities compared to higher order modes. The chosen numerical values of the core refractive index n_f are (1.90, 2.0, and 2.10) (Butt et al. 2022b). The practical values of the cover refractive indices n_c were selected as (1.4394, 1.47, and 1.501); these are corresponding to the glucose solution, vegetable oil and benzene materials, respectively. Noting that other materials of the cover can be chosen if their refractive indices are lower than those of the core and substrate. The appropriate core thicknesses will be determined based on the cut-off condition of the modes in each case. The temperature range considered in our study extends from 20 to 500 °C.

Figure 2 represents the sensitivity variation of the TE_0 (blue curves) and TM_0 (red curves) modes as a function of the temperature for different wavelengths of the source, solid lines for the source wavelength of 1550 nm and dashed lines for the source wavelength of 632.8 nm. The Figure demonstrates that the TM_0 mode exhibits higher sensitivities compared to the TE_0 mode. Additionally, the sensitivities decrease as the temperature increases. It should be noted that the selected core thickness is optimized for the source wavelength of 1550 nm, resulting in higher sensitivities for this wavelength compared to the source wavelength of 632.8 nm, this is true for both TE and TM polarizations.

It is worth to note that during the subsequent study, we will use a source with the wavelength of 1.55 μm. This choice is made based on technical considerations, since it is generally more practical to manufacture waveguides with larger thicknesses rather than those with smaller thicknesses. Knowing that longer wavelengths require greater core thicknesses and vice versa.

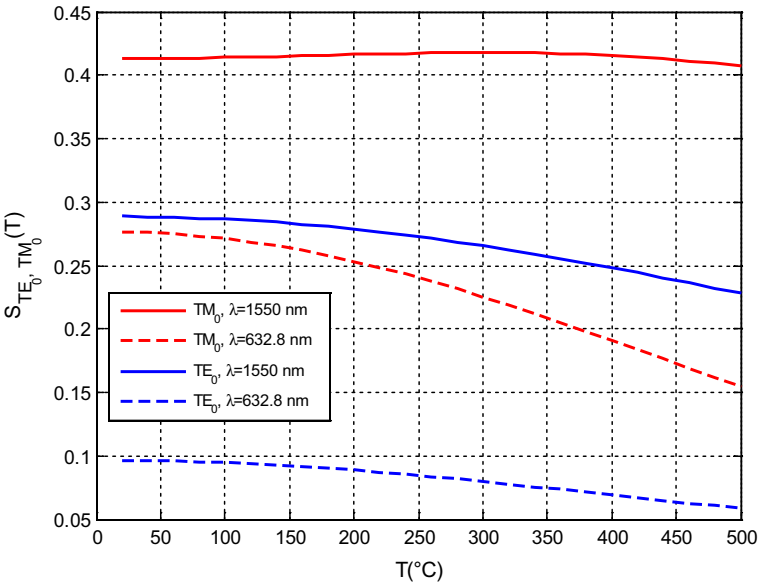

Fig. 2 Variation of the sensitivities of the TM_0 and TE_0 modes according to the temperature for different source wavelengths ($n_f = 2.10$, $n_c = 1.501$, $d_0 = 167$ nm)

3.1 Sensitivity temperature-dependence of TM modes in multimode structure

3.1.1 Random choice of waveguide parameters

In this section, we will first examine the case where only the TE_0 and TM_0 modes exist. We will specifically focus on the sensitivity of the TM_0 mode, as it exhibits greater sensitivity compared to the TE_0 mode. We aim to investigate how the sensitivities of the TM_0 mode vary with temperature, considering different random, physical and geometric parameters of the waveguide. Next, we will study the case of the TM_1 mode. It is important to note that the chosen core thicknesses satisfy the multimode condition specified by Eq. (6), for TM_0 and TM_1 modes.

Figures 3, 4 and 5 represent the variation of the sensitivities of the TM_0 mode as a function of the temperature for different core refractive indices, measurand refractive indices and core thicknesses, successively. It should be noted that the chosen core thickness for each figure satisfies the mode propagation condition. In fact, Figs. 3 and 4 show an increase in the sensitivities by increasing the refractive indices of the core and substrate. Whereas, Fig. 5 demonstrates that the sensitivities decrease as the core thicknesses increase. On the other hand, the curves indicate that the increase in the temperature leads to a diminution in sensitivities, particularly at high temperatures. It should be emphasized that this decrease in the sensitivity, as the temperature increases, is more pronounced for the higher values of the waveguide parameters. The difference between the maximum and minimum value of the sensitivity reaches 0.1, in some cases. These figures confirm that the arbitrary selection of the physical and geometrical parameters of the waveguide can have a significant impact on the sensitivity of the sensors and their variation with respect to the temperature.

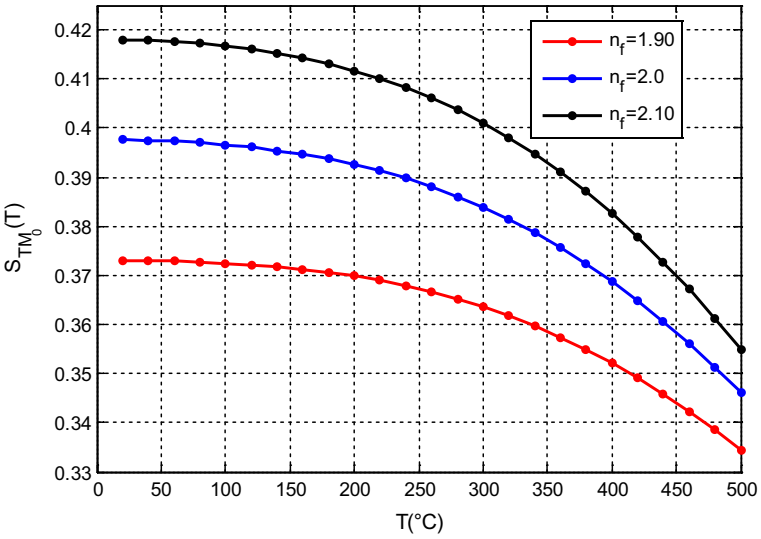

Fig. 3 Variation of the sensitivities of the TM_0 mode according to the temperature for different core refractive indices ($\lambda = 1550$ nm, $n_c = 1.501$, $d_0 = 230$ nm)

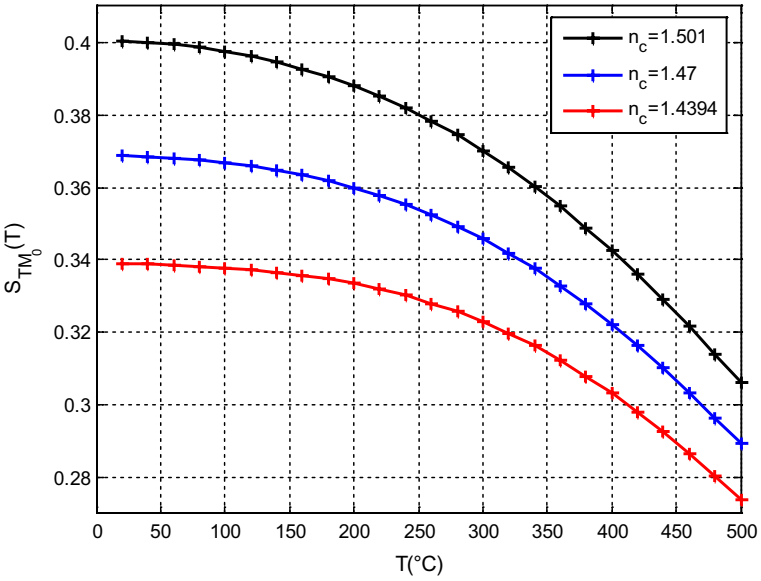

Fig. 4 Variation of TM_0 mode sensitivities as a function of the temperature for different cover refractive indices ($\lambda = 1550$ nm, $n_f = 2.1$, $d_0 = 270$ nm)

3.1.2 Optimization of the waveguide parameters

3.1.2.1 Case of TM_0 mode for different core refractive indices In order to increase the sensitivity of the sensor and to minimize the effect of the temperature, we have chosen optimal

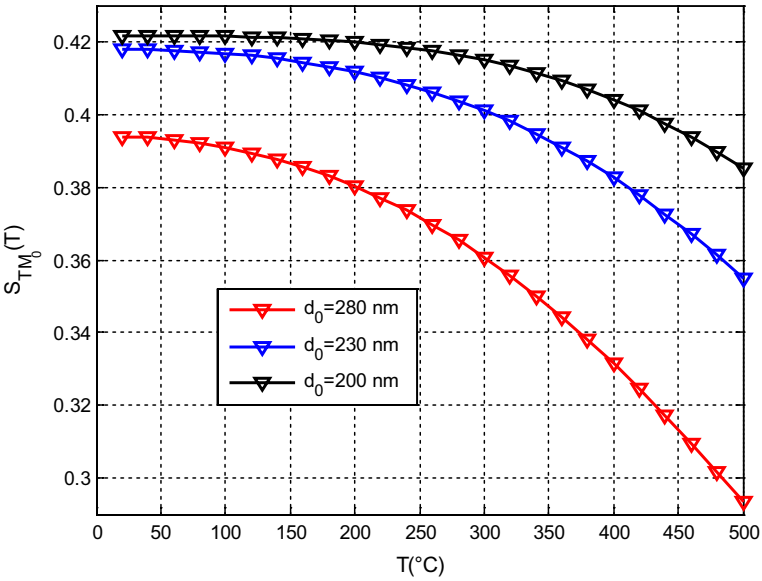

Fig. 5 Variation of TM_0 mode sensitivities as a function of the temperature for different core thicknesses ($\lambda = 1550$ nm, $n_f = 2.1$, $n_c = 1.501$)

thicknesses for each refractive index of the core. These thicknesses are those where the sensitivities are maximum at the starting temperature T = 20 °C, and the thicknesses close to the cut-off thicknesses of the TM_0 mode.

Through the plot of the sensitivity versus core thicknesses at the temperature of 20 °C, and for various values of core refractive indices, we sought to identify the core thicknesses (d_{0max}) those yield maximum sensitivities. According to the Fig. 6, these are 223 nm, 210 nm and 200 nm, corresponding to the core refractive indices of 1.9 (red curve), 2.0 (blue curve) and 2.1 (black curve), respectively.

Figure 7 presents the variation of the maximum sensitivities of the TM_0 mode as a function of the temperature for different values of the core refractive indices and the corresponding core thicknesses determined previously. The most prominent observation in this figure is that the sensitivities of the TM_0 mode, across all three-core refractive indices, decrease in the same manner and magnitude, as the temperature increases. However, the decrease in sensitivity is more important at higher temperatures. The difference between the maximum and minimum sensitivity values is 0.035, for all three curves. Nevertheless, this difference in sensitivities is relatively smaller compared to the cases where core thicknesses were randomly chosen. It is worth noting that below 100 °C, the sensitivities remain constant, while, beyond this temperature, they progressively decrease.

To achieve an improved stability of the sensitivity across the investigated temperature range, we have plotted the sensitivities for core thicknesses close to the cut-off thicknesses (d_{0min}) of the TM_0 mode. Specifically, we considered core thicknesses of 202 nm, 182 nm and 167 nm, corresponding to the core refractive indices 1.9, 2 and 2.1, respectively. The Fig. 8 exhibits nearly stable sensitivity curves across a wide temperature range (250 °C, 350 °C and 450 °C) for the respective core thicknesses of 202 nm, 182 nm and 167 nm. Furthermore, the sensitivities decrease for high temperatures are relatively smaller than that observed in the previous Fig. 7. The differences between the maximum and minimum

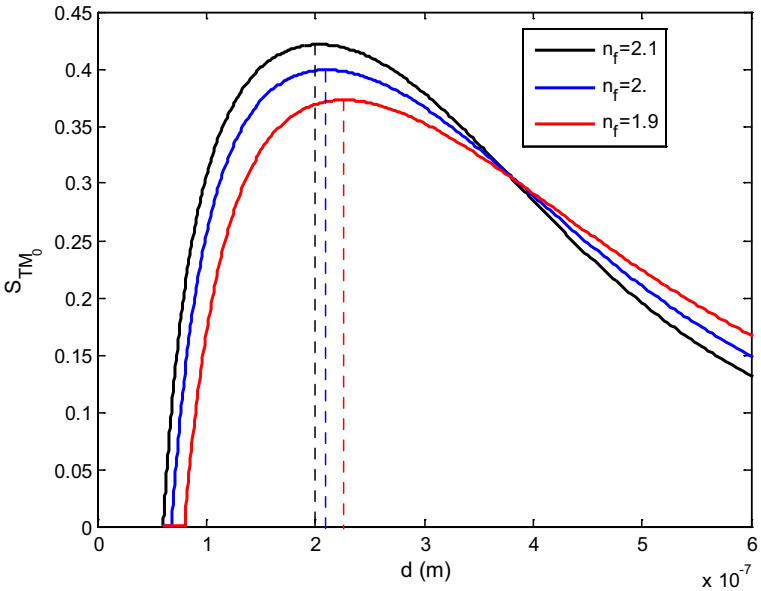

Fig. 6 Sensitivities of the TM_0 mode according to the core thicknesses for different core refractive indices at T = 20 °C (λ = 1550 nm, n_c = 1.501)

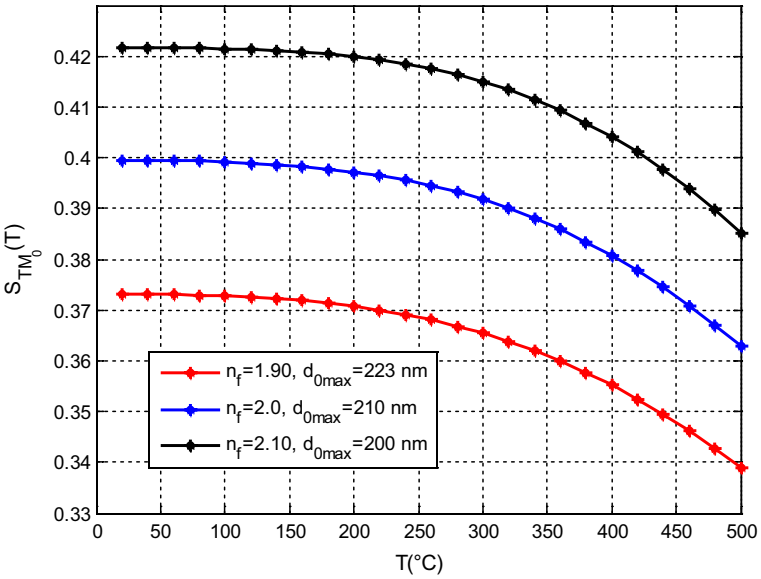

Fig. 7 Temperature dependence of the sensitivities of the TM_0 mode for different core refractive indices and for d_{0max} (λ = 1550 nm, n_c = 1.501)

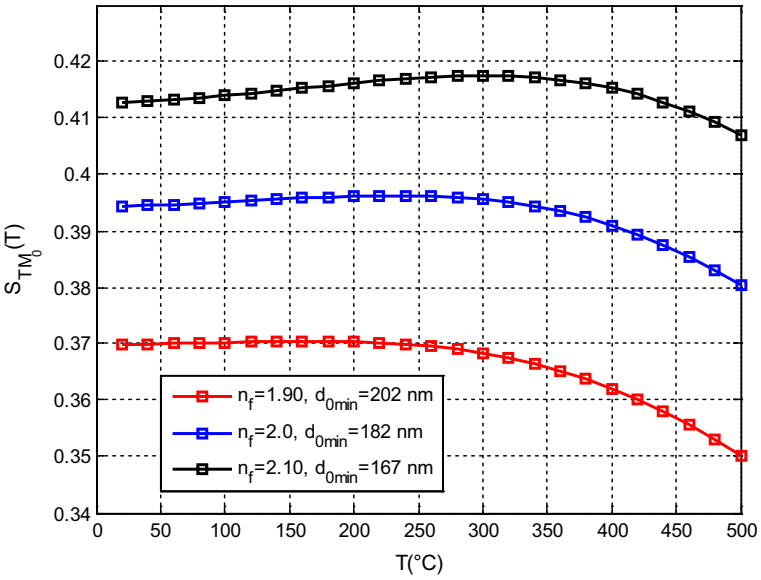

Fig. 8 Temperature dependence of the sensitivities of the TM_0 mode for different core refractive indices and for d_{0min} ($\lambda = 1550$ nm, $n_c = 1.501$)

value of the sensitivity are 0.005, 0.015 and 0.02, corresponding to the core refractive indices 2.1, 2 and 1.9, respectively. It is worth mentioning, that the curve for the largest core refractive index is the most stable.

3.1.2.2 Case of TM_0 mode for different cover refractive indices In this section, we will determine the optimal cover refractive index that provides the highest and most stable sensitivity as well as the conditions under which it occurs. The studied cover refractive indices are 1.501, 1.47 and 1.4394, while the used core refractive index is the highest (2.1), as it gives the best sensitivity. Firstly, we will identify the optimal thicknesses that result in the maximum sensitivities for each cover refractive index. These thicknesses are defined from Fig. 9, which displays the sensitivities of the TM_0 mode as a function of the thicknesses for three values of the measurand refractive indices. The deduced optimum thicknesses are 202.1 nm, 240.3 nm and 262.1 nm corresponding to the cover refractive indices of 1.501 (black curve), 1.47 (blue curve) and 1.4394 (red curve), respectively. Noting that, the highest sensitivity is achieved for the highest refractive index of the measurand, as it is closer to the substrate refractive index $n_s = 1.5254$. This proximity of refractive indices enhances the interaction between the waveguide and the surrounding medium, leading to a higher sensitivity of the sensor (Cherouana et al. 2019).

In Fig. 10, the sensitivity of the TM_0 mode is presented as a function of the temperature, for different values of the measurand refractive indices, and for the core thicknesses that provide maximum sensitivities. The Figure shows that the sensitivities exhibit a similar decreasing trend when the temperature increases, but with different magnitudes. Notably, the measurand refractive index with the highest value exhibits the slowest rate of sensitivity decrease. The differences between the maximum and minimum value of the sensitivity are 0.04, 0.055 and 0.06, corresponding to the measurand refractive indices 1.501, 1.47 and 1.4394, respectively.

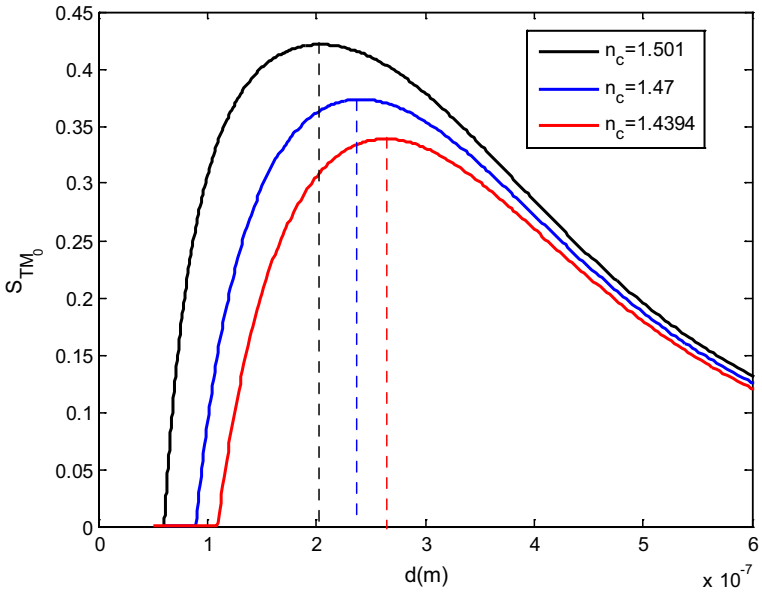

Fig. 9 Sensitivities of the TM_0 mode as a function of the core thicknesses for different cover refractive indices at T = 20 °C (λ = 1550 nm, n_f = 2.1)

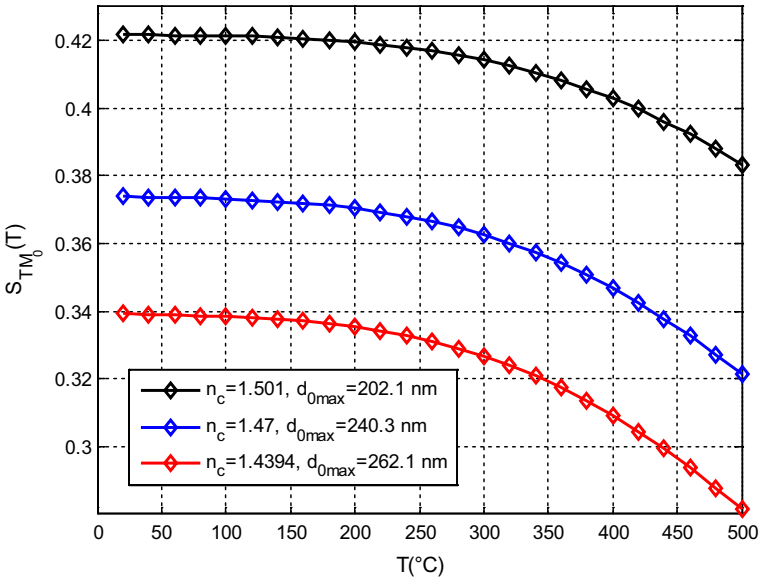

Fig. 10 Temperature dependence of the sensitivities of the TM_0 mode for different cover refractive indices and for d_{0max} (λ = 1550 nm, n_f = 2.1)

On the other hand, we also examined the temperature dependence of the sensitivity at different cover refractive indices, for core thicknesses close to the cut-off thicknesses of the TM_0 mode (see Fig. 11). These thicknesses are 167 nm, 170 nm and 174 nm, corresponding to the cover refraction indices of 1.501, 1.47 and 1.4394, respectively. In the case of a measurand refractive index of 1.501, the sensitivity remained relatively stable at around 0.41. However, for measurand refractive indices of 1.47 and 1.4394, the sensitivities increased with temperature. The Fig. 11 also indicates that the sensitivity increases and tends towards stabilization by increasing the measurand refractive index, provided that the latter is lower than the refractive index of the substrate.

3.1.2.3 Case of TM_1 mode for different core refractive indices Figure 12 illustrates the change in the sensitivities as a function of the temperature for the TM_1 mode, for three core refractive indices and their thicknesses corresponding to the maximum sensitivities. The figure shows that the sensitivities are maximum and almost stable at low temperatures (< 100 °C). However, they rapidly decrease as the temperature increases. Moreover, the curves indicate that, the higher core refractive indices result in a faster drop in sensitivity. The differences between the maximum and minimum sensitivities are 0.135, 0.12 and 0.105 for the core refractive indices of 2.1, 2 and 1.9, respectively. This emphasizes that the decrease in sensitivities with temperature is more pronounced for the mode TM_1 compared to the TM_0 mode.

In Fig. 13, the temperature dependence of the sensitivities for TM_1 mode are plotted considering core thicknesses near to the cut-off thicknesses of the TM_1 mode. The figure reveals that the sensitivities initially increase with temperature until reaching certain threshold values, after which they slowly decrease. It should be noted that the sensitivity values at low temperatures are very small.

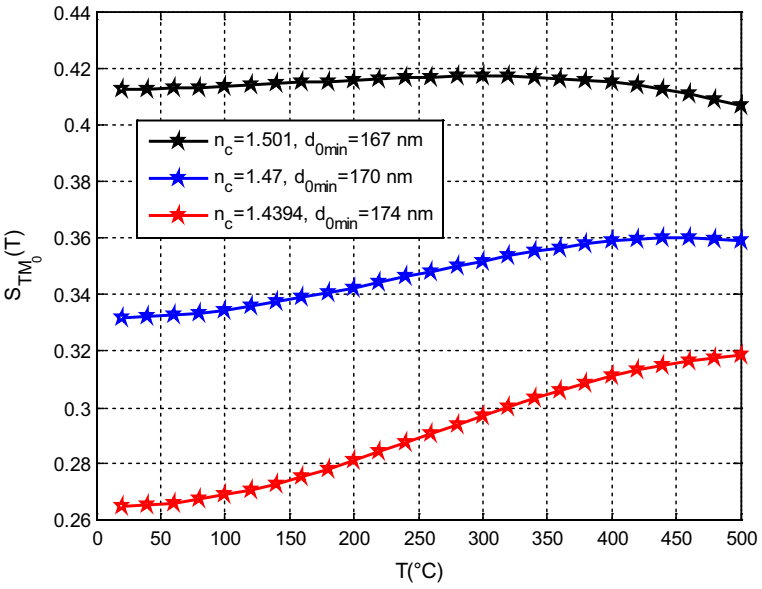

Fig. 11 Temperature dependence of the sensitivities of the TM_0 mode for different cover refractive indices and for d_{0min} ($\lambda = 1550$ nm, $n_f = 2.1$)

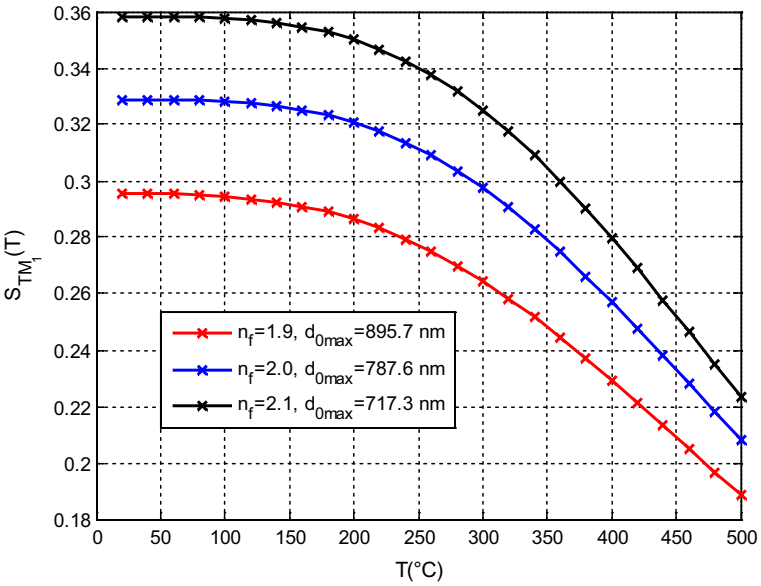

Fig. 12 Temperature dependence of the sensitivities of the TM_1 mode for different core refractive indices and for d_{0max} ($\lambda = 1550$ nm, $n_c = 1.501$)

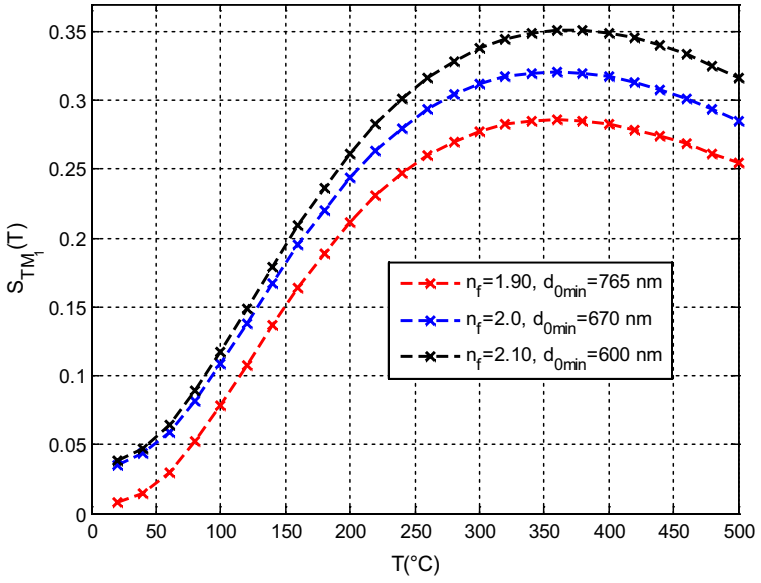

Fig. 13 Temperature dependence of the sensitivities of the TM_1 mode for different core refractive indices and for d_{0min} ($\lambda = 1550$ nm, $n_c = 1.501$)

3.2 Sensitivity temperature-dependence of TE_0 mode in single mode structure

In this case, we will focus on the TE_0 mode as the only propagating mode. We aim to investigate whether the behavior of the TE_0 single mode is similar to that of the TM_0 mode, regarding the variation of sensitivity with temperature for different physical and geometric parameters of the waveguide.

As in the case of TM_0 mode, we have chosen optimal thicknesses for each refractive indices of the core and the cover. These thicknesses are those where the sensitivities are maximum at the starting temperature T = 20 °C, and the thicknesses close to twice the cut-off thicknesses of the TE_0 mode. The choice of twice the cut-off thicknesses for the TE_0 mode is a result of simulation; in fact, we have plotted S versus T for different values of thickness (d), far and close to the cut-off thicknesses of the TE_0 mode. Our findings indicate that employing a thickness (d) approximately double the cut-off value yields the highest and most stable sensitivity.

3.2.1 Case of TE_0 mode for different core refractive indices

Firstly, the optimal core thicknesses (d_{0max}) those yield maximum sensitivities at T = 20 °C are deduced from Fig. 14, these are 130 nm, 100 nm and 86.72 nm, corresponding to the core refractive indices of 1.9 (red dashed curve), 2.0 (blue dashed curve) and 2.1 (black dashed curve), respectively.

Figure 15 depicts the sensitivity change of the TE_0 mode with respect to the temperature for different core refractive indices and for the thicknesses d_{0max} defined previously. The figure shows that the sensitivities decrease with increasing temperature but not at the

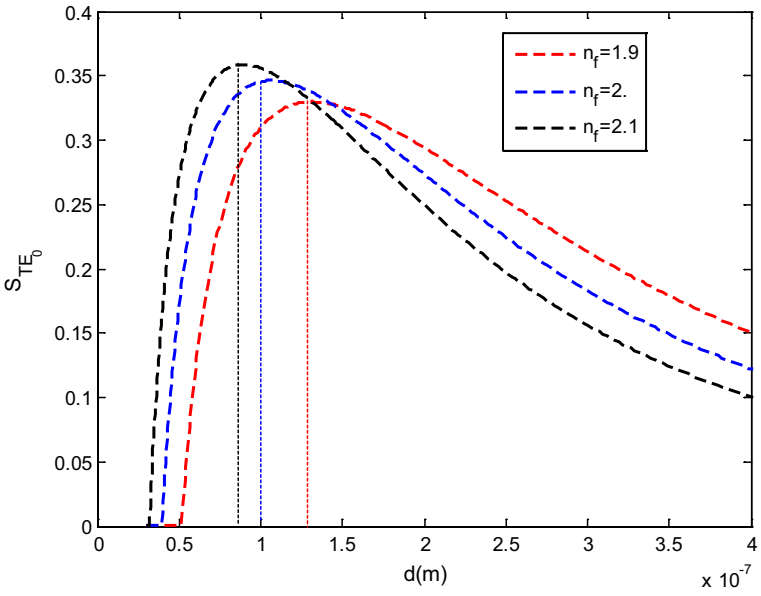

Fig. 14 Sensitivities of the TE_0 mode as a function of the core thicknesses for different core refractive indices at T = 20 °C (λ = 1550 nm, $n_c = 1.501$)

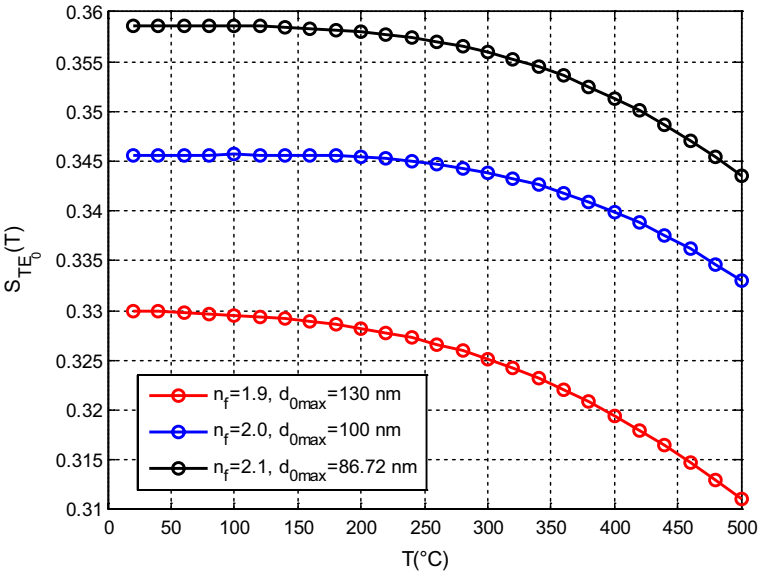

Fig. 15 Temperature dependence of the sensitivities of the TE_0 mode for different core refractive indices and for d_{0max} ($\lambda = 1550$ nm, $n_c = 1.501$)

same rate for all cases. Notably, the sensitivity with the core refractive index 2.0 exhibits the widest stabilization range, extending up to 200 °C. Beyond this temperature, there is a decrease of 0.0125 compared to the initial value of sensitivity. For the core refractive index of 2.1, the sensitivity stabilization persists up to 150 °C, followed by a decrease of 0.015 at 500 °C. Whereas, the difference between the maximum and minimum value of the sensitivity is almost 0.02, corresponding the core refractive index value of 1.9. It can be observed that the decrease in sensitivities of the TE_0 mode with increasing temperature, are small, compared to those of the TM_0 mode. This suggest that the TE_0 mode is less affected by temperature variation, making it more suitable for certain applications where temperature stability is crucial.

In order to enhance sensitivities at elevated temperatures, we have presented in Fig. 16, the sensitivities corresponding to core thicknesses close to twice the cut-off thicknesses of the TE_0 mode, considering various core refractive indices. The plotted curves reveal that as temperature rises, the sensitivities exhibit a notable increase, especially for higher core refractive indices.

3.2.2 Case of TE_0 mode for different cover refractive indices

As in the previous case, the core thicknesses (d_{0max}) corresponding the maximum sensitivities at T = 20 °C, are deduced from Fig. 17, these are 124.5 nm, 111.3 nm and 89.96 nm, for the cover refractive indices of 1.4394 (red dashed curve), 1.47 (blue dashed curve) and 1.501 (black dashed curve), respectively.

The temperature-dependent sensitivities of the mode TE_0 are depicted in Fig. 18 for various refractive indices of the measurand. The core thicknesses (d_{0max}) chosen for analysis are those determined previously. Notably, the curves appear to be identical and the sensitivity gradually decreases with increasing temperature. The difference between the

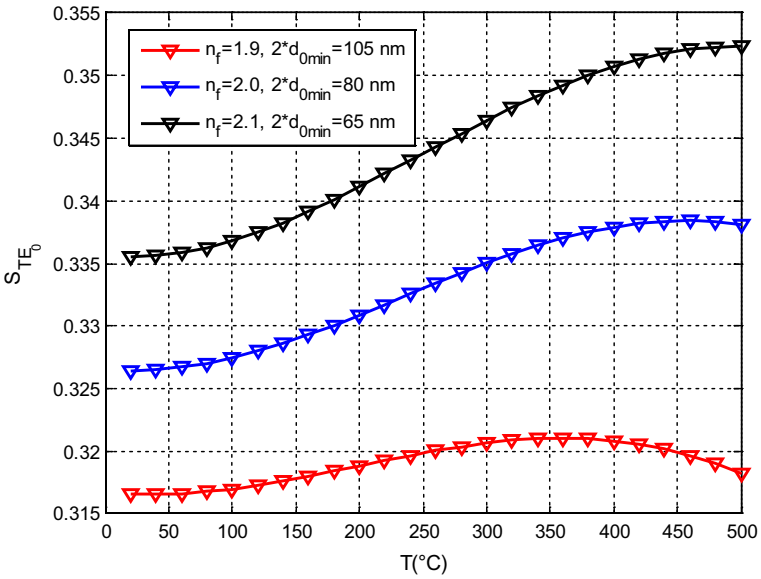

Fig. 16 Temperature dependence of the sensitivities of the TE_0 mode for different core refractive indices and for $2*d_{0min}$ ($\lambda = 1550$ nm, $n_c = 1.501$)

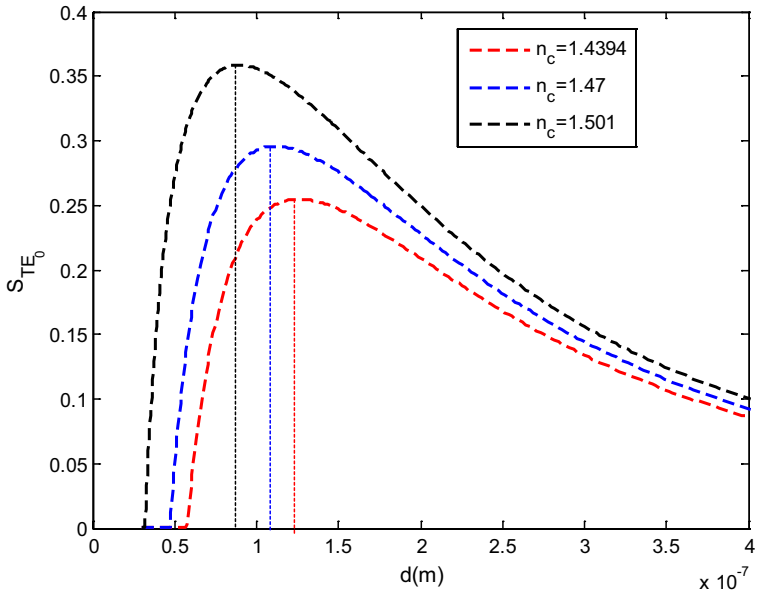

Fig. 17 Sensitivities of the TE_0 mode as a function of the core thicknesses for different cover refractive indices at T = 20 °C ($\lambda = 1550$ nm, $n_f = 2.1$)

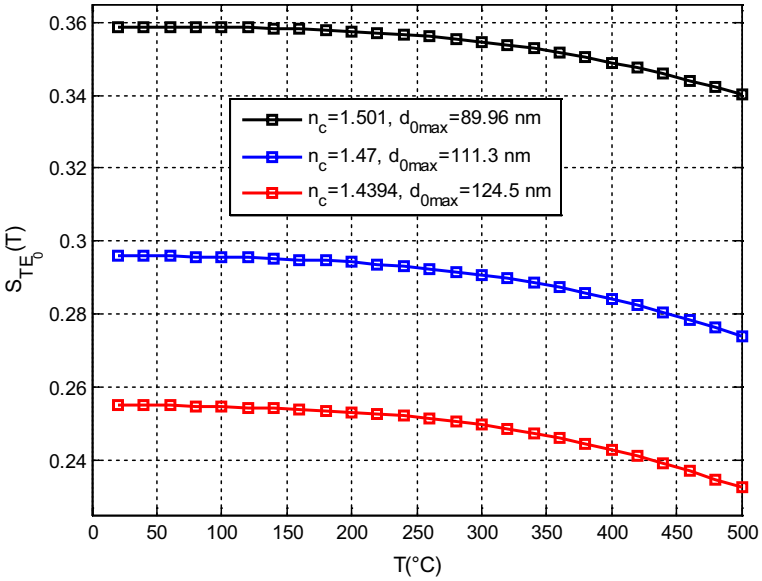

Fig. 18 Temperature dependence of the sensitivities of the TE_0 mode for different cover refractive indices and for d_{0max} ($\lambda = 1550$ nm, $n_f = 2.1$)

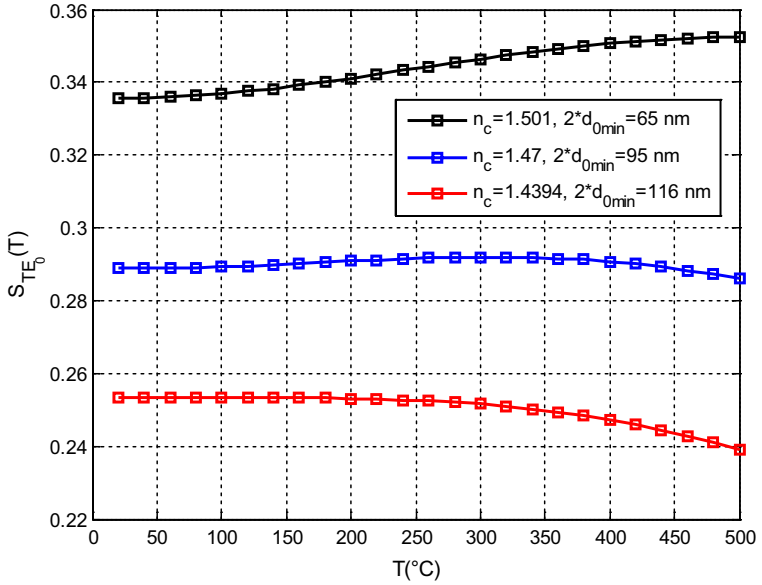

Fig. 19 Temperature dependence of the sensitivities of the TE_0 mode for different cover refractive indices and for $2*d_{0min}$ ($\lambda = 1550$ nm, $n_f = 2.1$)

maximum and minimum sensitivity is 0.02, indicating acceptable stability. Furthermore, Fig. 19 illustrates the sensitivity plot for core thicknesses near twice the cut-off thicknesses corresponding to each refractive index of the measurand. This approach yields even more

Table 1 Summarizing of the best numerical results obtained for different modes

Modes	The highest and most stable sensitivity	n_f	n_c	Optimized thicknesses d_0 (nm)
TM_0	Around of 0.41	2.1 (the highest)	1.501 (the closest to n_s)	d_{0min} (167) ≤ d_{opt} ≤ d_{0max} (200)
Single TE_0	Around of 0.35	2.1 (the highest)	1.501 (the closest to n_s)	2* d_{0min} (65) ≤ d_{opt} ≤ d_{0max} (86.72)

favorable results, particularly in terms of sensitivity stabilization. Specifically, for a cover refractive index of 1.501, the sensitivity exhibits a slightly increase with temperature. Conversely, for a cover refractive index equals to 1.4394, the sensitivity experiences a slight decrease of approximately 0.015. Nevertheless, the sensitivity remains nearly constant at around 0.29, for a cover refractive index of 1.47.

Table 1 summarizing the best numerical results obtained for different modes, including the highest and more stable values of the sensitivities, their optimized thicknesses and their corresponding refractive indices.

4 Conclusion

In summary, this study demonstrates that the random choice of physical and geometrical parameters of the waveguide could significantly decrease the sensitivity of the sensor as the temperature increases. However, the appropriate selection of these parameters, particularly, the core thickness, not only made it possible to increase the sensitivity but also to extend its range of stabilization with respect to the temperature, and in certain cases the sensitivity could even be notably enhanced with rising the temperature. The most favorable results, in terms of sensitivity value and stability are obtained, by selecting a larger core refractive index with a measurand refractive index closest to that of the substrate. Regarding the geometrical parameters, optimal results can be achieved for the core thicknesses located between the core thickness where the sensitivity is maximum at room temperature and the cut-off thickness of the TM_0 mode. Similarly, for the single mode structure, the best results can be attained for core thicknesses positioned between the thickness where the sensitivity is maximum at room temperature and twice the cut-off thickness of the TE_0 single mode. This study demonstrate that the SiO_2:TiO_2 waveguide based optical sensor can be used in high temperature environment with high and quasi-stable sensitivity, provided that the waveguide's parameters are suitably defined. This holds true for both TE and TM polarizations.

Author contributions All authors contributed to the study conception and design. AC wrote the first draft of the manuscript. AB and IB provided guidance and supervision. All authors reviewed and commented on previous versions of the manuscript. All authors read and approved the final manuscript**.**

Funding This research received no external funding**.**

Data availability Not applicable.

Declarations

Conflict of interest The authors declare no conflict of interest.

Ethical approval Not applicable.

References

Butt, M.A., Kazmierczak, A., Tyszkiewicz, C., Karasinski, P., Piramidowicz, R.: Mode sensitivity exploration of silica-titania waveguide for refractive index sensing applications. Sensors **21**(22), 7452 (2021a). https://doi.org/10.3390/s21227452

Butt, M.A., Tyszkiewicz, C., Karasinski, P., Zieba, M., Kazmierczak, A., Zdonczyk, M., Duda, L., Guzik, M., Olszewski, J., Martynkien, T., Bachmatiuk, A., Piramidowicz, R.: Optical thin films fabrication techniques: towards a low-cost solution for the integrated photonic platform. Rev. Curr. Stat. Mater. **4591**(15), 1–25 (2022a). https://doi.org/10.3390/ma15134591

Butt, M.A., Tyszkiewicz, C., Karasinski, P., Zieba, M., Hlushchenko, D., Baraniecki, T., Kazmierczak, A., Piramidowicz, R., Guzik, M., BachmatiuK, A.: Development of a low-cost silica–titania optical platform for integrated photonics applications. Opt. Express. **13**(30), 23678–23694 (2022b). https://doi.org/10.1364/OE.460318

Butt, M.A., Shahbaz, M., Kozlowski, L., Kazmierczak, A., Piramidowicz, L.: Silica titania integrated photonics platform-based 1 × 2 demultiplexer utilizing two serially cascaded racetrack microrings for 1310 nm and 1550 nm telecommunication wavelengths. Photonics **10**, 208 (2023). https://doi.org/10.3390/photonics10020208

Butt, M.A., Kozlowski, L., Piramidowicz, R.: Numerical scrutiny of silica–titania-based reverse rib waveguide with vertical and rounded side walls. Optica Publishing Group. https://opg.optica.org/ao/abstract.cfm?uri=ao-62-5-1296 (2021b)

Chekhlova, T.K., Zhivtsov, S.V., Grabovskii, E.I.: Temperature dependence of sol–gel waveguides. J. Commun. Technol. Electron. **7**(51), 804–809 (2006). https://doi.org/10.1134/S1064226906070114

Chen, C.-L.: Foundations for Guided-Wave Optics. Wiley, Hoboken (2007)

Cherouana, A., Bencheikh, A., Bouchama, I.: Effect of the electric field induced birefringence on the slab waveguide evanescent wave sensor sensitivity. Opt. Quantum Electron. **51**, 331 (2019). https://doi.org/10.1007/s11082-019-2018-2

Chiavaioli, F., Biswas, P., Trono, C., Jana, S., Bandyopadhyay, S., Basumallick, N., Giannetti, A., Tombelli, S., Bera, S., Mallick, A., Baldini, F.: Sol-gel based titania–silica thin film overlay for long period fiber grating-based biosensors. Anal. Chem. **87**(24), 12024–12031 (2015). https://doi.org/10.1021/acs.analchem.5b01841

Dhall, S., Mehta, B.R., Tyagi, A.K., Sood, K.: A review on environmental gas sensors: materials and technologies. Sens. Int. **2**, 100116 (2021). https://doi.org/10.1016/j.sintl.2021.100116

Farhad, M.H., Sagor, R.H., Infiter, T., Kazi, S.R., Radoan, M.: An optimized dielectric-metal-dielectric refractive index nanosensor. IEEE Sens. J. **21**(2), 1461–1469 (2017). https://doi.org/10.1109/JSEN.2020.3016570

Farhad, M.H., Infiter, T., Radoan, M., Sagor, R.H.: A concentric double-ring resonator based plasmonic refractive index sensor with glucose sensing capability. IN: 2020 IEEE Region 10 Conference (TENCON) Osaka, Japan, November 16–19 (2020). https://doi.org/10.1109/TENCON50793.2020.9293901

Fomekong, R.L., Saruhan, B.: Titanium based materials for high-temperature gas sensor in harsh environment application. Chem. Proc. **5**(1), 66 (2021). https://doi.org/10.3390/CSAC2021-10480

Ghosh, A., Zhang, C., Shi, S.Q., Zhang, H.: Review High-Temperature Gas Sensors for Harsh Environment Applications. Wiley, Weinheim (2019). https://doi.org/10.1002/clen.201800491

Infiter, T., Ahmed, A.Y., Kazi, S.R., Sagor, R.H.: Metal-insulator-metal waveguide-based optical pressure sensor embedded with arrays of silver nanorods. Opt. Express **29**, 32365–32376 (2021a). https://doi.org/10.1364/OE.439974

Infiter, T., Kazi, S.R., Ahmed, A.Y., Sagor, R.H.: Alternative material titanium nitride based refractive index sensor embedded with defects: an emerging solution in sensing arena. Res. Phys. **29**, 104795 (2021b). https://doi.org/10.1016/j.rinp.2021.104795

Infiter, T., Farhad, M.H., Kazi, S.R., Ahmed, A.Y., Sagor, R.H.: A highly sensitive plasmonic refractive index sensor based on concentric triple ring resonator for cancer biomarker and chemical concentration detection. Opt. Commun. (2022). https://doi.org/10.1016/j.optcom.2022.128429

Islam, S., Bakhtiar, H., Bidin, N., Salim, A.A., Riaz, S., Krishnan, G., Naseem, S.: Crack-free high surface area silica–titania nanocomposite coating as opto-chemical sensor device. Sens. Actuators A: Phys. **270**, 153–161 (2018). https://doi.org/10.1016/j.sna.2017.12.063

Islam, S., Bakhtiar, H., Haider, Z., Alshoaibi, A., Riaz, S., Naseem, S.: Silica–titania nanocomposite based fiber optic sensor for aromatic hydrocarbons detection. Opt. Commun. **471**, 125825 (2020). https://doi.org/10.1016/j.optcom.2020.125825

Karasinski, P., Tyszkiewicz, C., Rogozinski, R., Jaglarz, J., Mazur, J.: Optical rib waveguides based on sol–gel derived silica–titania films. Thin Solid Films **16**(519), 5544–5551 (2011). https://doi.org/10.1016/j.tsf.2011.02.064

Karker, N., Dharmalingam, G., Carpenter, M.A.: Harsh environment compatible plasmonics based chemical sensors. Advanced Photonics Congress (IPR, Networks, NOMA, PS, Sensors, SPPCom)© OSA 2017

Kazi, S.R., Infiter, T., Ahmed, A.Y., Farhad, M.H., Sagor, R.H.: Cog-shaped refractive index sensor embedded with gold nanorods for temperature sensing of multiple analytes. Opt. Express **29**(23), 37541–37554 (2021a). https://doi.org/10.1364/OE.442954

Kazi, S.R., Farhad, M.H., Ahmed, A.Y., Infiter, T., Sagor, R.H.: Gas-sensing and label-free detection of biomaterials employing multiple rings structured plasmonic nanosensor. Sens. Bio-Sens. Res. **33**, 100440 (2021b). https://doi.org/10.1016/j.sbsr.2021.100440

Morosanova, E.I.: Silica and silica–titania sol–gel materials: synthesis and analytical application. Talanta **102**, 114–122 (2012). https://doi.org/10.1016/j.talanta.2012.07.043

Morosanova, M.A., Morosanova, E.I.: Silica–titania sensor material prepared by cetylpyridinium chloride assisted sol-gel synthesis for solid phase spectrophotometric and visual test determination of propyl gallate in food samples. Anal. Methods (2016). https://doi.org/10.1039/C6AY02473D

Nikolaev, N.E., Pavlov, S.V., Trofimov, N.S., Chekhlova, T.K.: Analysis of the temperature coefficient of effective refractive index of the TE_1 and TM_1 modes in optical sol–gel waveguides. J. Commun. Technol. Electron. **1**(57), 15–21 (2012a). https://doi.org/10.1134/S1064226912010135

Nikolaev, N.E., Pavlov, S.V., Trofimov, N.S., Chekhlova, T.K.: The temperature dependence of the effective refractive index of TE_1 and TM_1 modes in optical sol–gel waveguides over a wide temperature range. J. Russ. Laser Res. **6**(33), 536–541 (2012b). https://doi.org/10.1007/s10946-012-9312-9

Nikolaev, N.E., Pavlov, S.V., Chekhlova, T.K.: Features of propagation of electromagnetic waves in sol–gel optical waveguides under varying temperature. J. Commun. Technol. Electron. **11**(63), 1265–1268 (2018). https://doi.org/10.1134/S1064226918110074

Parrino, F., Palmisano, L.: Titanium dioxide (Tio_2) and its applications: a volume in metal oxides. Elsevier Inc (2021). https://doi.org/10.1016/C2019-0-01050-3

Pavlov, S.V., Trofimov, N.S., Chekhlova, T.K.: Investigation of the temperature coefficient of the effective refractive index of optical sol–gel waveguides using a peltier module. Optoelectron. Instrum. Data Process. **3**(49), 313–319 (2013). https://doi.org/10.3103/S875669901303014X

Pavlov, S.V., Trofimov, N.S., Chekhlova, T.K.: Integrated optical devices based on sol-gel waveguides using the temperature dependence of the effective refractive index. Quantum Elec. **7**(44), 703–706 (2014). https://doi.org/10.1070/QE2014v044n07ABEH015179

Sainit, S., Kurratt, R., Prenosilt, J.E., Ramsden, J.J.: Temperature dependence of pyrolysed sol–gel planar waveguide parameters. J. Phys. D: Appl. Phys. **6**(27), 1134–1138 (1994). https://doi.org/10.1088/0022-3727/27/6/009

Tiefenthaler, K., Lukosz, W.: Sensitivity of grating couplers as integrated-optical chemical sensors. J. Opt. Soc. Am. B. **2**(6), 209–220 (1989). https://doi.org/10.1364/JOSAB.6.000209

Uniyal, A., Gaurav, S., Amrindra, P., Sofyan, T., Arjuna, M.: Recent advances in optical biosensors for sensing applications: a review. Plasmonics **18**, 735–750 (2023). https://doi.org/10.1007/s11468-023-01803-2